

Blind Manipulation of Deformable Linear Objects Based on Force Information from Environmental Contacts

Rita Laezza¹, Finn Süberkrüb, and Yiannis Karayiannidis¹

Abstract—Humans have the ability to manipulate Deformable Linear Objects (DLOs) such as cables, with little or no visual information by relying on force torque (FT) sensing. In this work, we propose a simplified graph representation of a DLO which enables such blind manipulation by keeping the object under tension. We show that our representation can be estimated online by a Kalman filter using FT data, which can then be used to define a set of sliding and clipping manipulation primitives. Both the estimation and manipulation primitives were tested, demonstrating that force-based perception can be sufficient for robotic tasks such as cable harness production.

I. INTRODUCTION

Force Torque (FT) sensing has been extensively used in robotic contact and interaction tasks both for feedback control schemes and for estimating important properties of the objects being manipulated [1]–[4]. However, most research has been limited to rigid objects, whose state can be summarized by their pose. Deformable objects constitute a still under-explored class of objects that often require more complex state representations, since such objects may also change in shape. Research on FT-based deformable object manipulation has been limited due to challenges in sensing, since FT measurements require the object to provide sufficient resistance to an applied force. This work focuses on objects much larger along one dimension than the other two dimensions, namely Deformable Linear Objects (DLOs) [5]. When manipulating a DLO, it will not offer resistance to deformation in any direction, unless it is under tension. This property is exploited to formulate our simplified graph representation and nine manipulation primitives.

Although visual and tactile sensing are also important in such contexts, here we aim to explore how far one can get with FT information alone. Sanchez et al. [6] proposed such a deformable object manipulation approach, but with a more complex model and for a problem without environmental contacts. Here we focus on tasks where the environment provides contacts which constrain the Degrees of Freedom (DOFs) of the DLO, such as cable harness problems. There have been few works exploring DLO manipulation with environmental contacts [7], [8], and these did not make use of FT sensing. Most notably, Zhu et al. [9] proposed a motion planning framework, using two motion primitives designed for a robot to shape a DLO through circular contacts. While they use a vision-based contact detector, we attempt to estimate contacts through FT information and make no assumptions on the shape of the contact surface.

¹Division of Systems and Control, Department of Electrical Engineering, Chalmers University of Technology, Sweden {laezza, yiannis}@chalmers.se

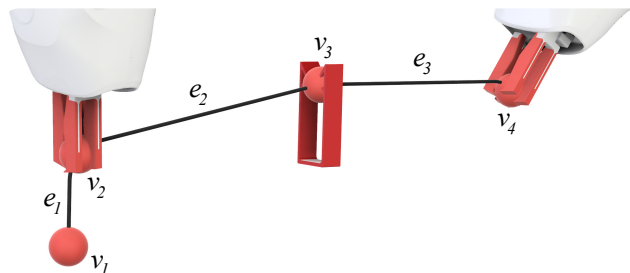


Fig. 1: Illustration of DLO model constrained by two YuMi SmartGrippers with four feature points v_1 to v_4 represented by red spheres and three edges e_1 to e_3 , represented as black lines.

II. PROBLEM STATEMENT

We address force-based manipulation of DLOs without complementary visual information, therefore the robot is assumed to be equipped with at least one wrist FT sensor capable of measuring the tension of the DLO. Furthermore, the problem is formulated assuming that once a DLO is gripped, its local pose is known. Consequently, the grippers must prevent involuntary slipping of the DLO along the x (red) and z (blue) axes, while also allowing a controlled sliding motion along x when desired. This can be achieved mechanically through specialized parallel grippers, shown in Fig. 2, which guide the DLO to a known location on the fingers and stop any further displacement along z .

In order to overcome the blindness of the robot, the workspace must satisfy one key condition, namely it must provide sufficient contact points in the form of fixtures or pivoting points, which restrict the DOFs of the DLO, thus enabling tensioning. This is imperative, since when a DLO is fully stretched between two points, the shape between them can be assumed linear. Note that gravity itself can be used to restrict the DOFs of the DLO. Once an end-effector equipped with a FT sensor is gripping the object by holding it limp in the air, the shape of the DLO segment below the gripper can be inferred to be vertical, assuming quasi-static motion.

III. DLO REPRESENTATION

We propose a model $\{\mathcal{G}, \rho\}$ to represent the state of a uniformly weighted DLO. While ρ is a known constant that denotes the DLO's weight per unit length, its state is modeled as a path graph $\mathcal{G} = (V, E)$ where: V is a set of feature points on the DLO which can be listed in the order $v_1, v_2, \dots, v_{|V|}$; and E is a set of edges connecting adjacent feature points, (v_i, v_{i+1}) for $i = 1, 2, \dots, |V| - 1$. Note that the cardinality of V , denoted by $|V|$, is not constant, and will change as the manipulator interacts with the DLO and indirectly with the environment.

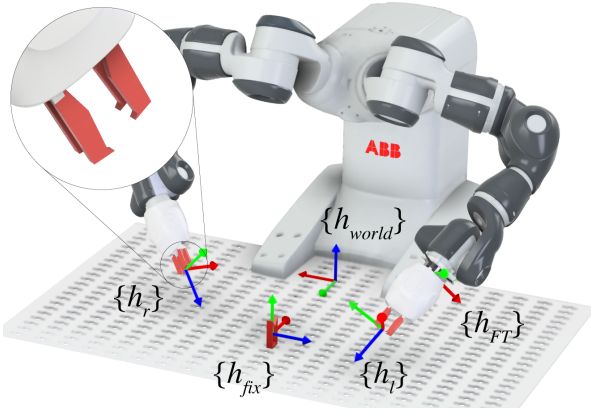


Fig. 2: Robotic setup of a YuMi equipped with specialized parallel grippers and one fixture attached to a pegboard. Relevant frames are indicated as: $\{h_{FT}\}$ - FT sensing frame, $\{h_l\}/\{h_r\}$ - left/right gripper tool tip frame, $\{h_{fix}\}$ - fixture frame, $\{h_{world}\}$ - world frame. Red, green and blue arrows indicate x -, y - and z -axes, respectively.

A. Feature Points, V

The i -th feature point describing the state of the DLO is defined as a tuple $v_i = (\mathbf{p}_i, \mathbf{Q}_i, m_i)$, where $\mathbf{p}_i \in \mathbb{R}^3$ is the position, \mathbf{Q}_i represents the orientation as a unit quaternion and $m_i \in \mathbb{R}$ is the mass.

If the feature point is the result of a perceived tension, it may be due to an unknown contact with the environment or another gripper. While in the first case \mathbf{p}_i must be estimated, in the latter it can be obtained directly through forward kinematics. Furthermore, if an additional feature point v_k is introduced to define a goal, it can be determined by linear interpolation between two neighboring points, v_{k-1} and v_{k+1} . The index k will depend on the location of the added point relative to the existing points in the model. The position is then calculated by interpolation as:

$$\mathbf{p}_k = \mathbf{p}_{k-1} + \delta(\mathbf{p}_{k+1} - \mathbf{p}_{k-1}), \text{ with } \delta \in [0, 1] \quad (1)$$

Since the orientation cannot be accurately estimated, it is only inferred from the pose of the gripper. For estimated points, the orientation is set so that the x -axis is aligned with the length of the DLO, without twist i.e. the orientation of two adjacent points is the same. When a point v_k is added to describe a goal, a linear interpolation between two quaternion orientations is computed by spherical linear interpolation, analogously to the position.

Finally, the mass of the DLO is equally distributed between the feature points, leading to m_i . Depending on the relative location of a feature point with respect to other points, the mass is computed as:

$$m_i = \begin{cases} \frac{d_i}{2} \rho & , i \text{ is an end-point of the DLO} \\ \frac{d_{i-1} + d_i}{2} \rho & , i \text{ is between feature points} \end{cases} \quad (2)$$

where d_i is a property of the edges to be described next.

B. Edges, E

The i -th edge, connecting two adjacent feature points (v_i, v_{i+1}) is defined as a tuple $e_i = (d_i, s_i, f_i, k_i)$, where $d_i \in \mathbb{R}$ describes the length, $s_i \in \mathbb{R}$ is the sag, $f_i \in \mathbb{R}$ the

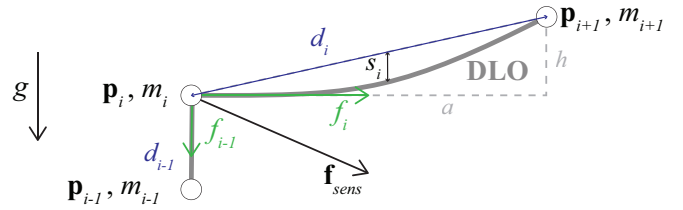


Fig. 3: Sag for edge with length d_i is denoted by s_i . The force measured by an FT sensor in rigid contact with feature point v_i is shown as \mathbf{f}_{sens} . The position \mathbf{p}_{i-1} and mass m_{i-1} can be determined using knowledge of \mathbf{p}_i and the measured force \mathbf{f}_{sens} . Force f_i is a result of the tension between \mathbf{p}_i and \mathbf{p}_{i+1} , while the force f_{i-1} is caused by the mass m_{i-1} .

tension and $k_i \in \mathbb{R}$ the spring constant of the DLO between feature point v_i and an adjacent feature point v_{i+1} .

The sag s_i between two feature points, illustrated in Fig. 3, is a measure used to determine whether the tensioning of the DLO is sufficient for the assumption of a linear connection. If two feature points are not on the same horizontal line and the sag-to-span ratio ($s/a \ll 1$) is small enough, no part of the DLO is below the lower feature point. In such cases, the sag can be approximated [10], unless one of the feature points is the extremity of the DLO, constrained by gravity alone, in which case the sag is set to 0.

The weight compensated DLO tension f_i between an end-effector at feature point v_i equipped with a FT sensor and a second feature point v_{i+1} can be calculated from the force measurements \mathbf{f}_{sens} and the preceding edge's tension f_{i-1} according to:

$$\hat{\mathbf{p}}_i f_i = \mathbf{f}_{sens} - \begin{bmatrix} 0 \\ 0 \\ g \end{bmatrix} m_i + \hat{\mathbf{p}}_{i-1} f_{i-1} \quad (3)$$

where g denotes the gravitational acceleration, and the unit vectors $\hat{\mathbf{p}}_{i-1}$ and $\hat{\mathbf{p}}_i$ denote the normalized force directions:

$$\hat{\mathbf{p}}_i = \frac{(\mathbf{p}_{i+1} - \mathbf{p}_i)}{\|\mathbf{p}_{i+1} - \mathbf{p}_i\|} \quad (4)$$

With only one FT sensor, the force f_{i-1} can only be taken into account under the assumption that it results from the mass of the rope (a free hanging feature point). In order to sense a second tension e.g. if the DLO is tensioned on both sides of the gripper, another FT sensor would be necessary.

IV. MANIPULATION PRIMITIVES

In this section we present a set of manipulation primitives for DLOs, which can be executed based on FT sensing alone, and limited knowledge about the environment. These are illustrated in Fig. 4, together with their description.

Each primitive specifies a desired force $f_d \in \mathbb{R}$, position $\mathbf{x}_d \in \mathbb{R}^3$ and quaternion orientation \mathbf{Q}_d as well as a projection matrix $\mathbf{P} \in \mathbb{R}^{12 \times 12}$ to define in which dimensions a force control is active. The primitives are divided into individual control primitives, where the two end-effectors are controlled separately, and coordinated control primitives, where the absolute and relative end-effector position is controlled. In both cases, a hybrid motion-force controller is used to compute the task space velocities [11].

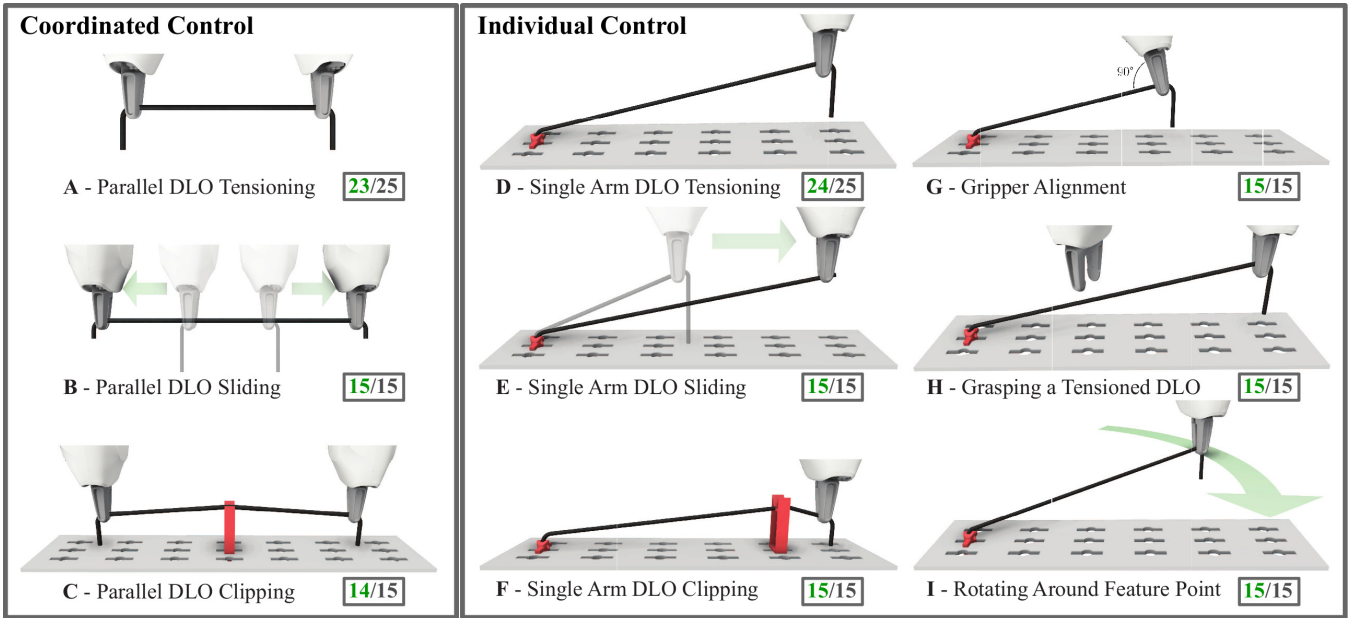


Fig. 4: FT-based manipulation primitives for DLO manipulation. These constitute diverse actions such as tensioning, clipping, sliding, grasping and rotating. Motion primitives are divided into individual and coordinated control, depending on whether or not the robot arms are controlled separately. The number of successful trials (green) from randomized states is shown for each primitive. Since tensioning primitives (A and D) are essential for the proposed DLO representation, these were tested for 25 trials, while the rest were tested for 15 trials.

V. EVALUATION

A dual-arm YuMi robot equipped with an ATI Mini40 6-axis FT sensor, was used in the real-world experiments. For a global evaluation of our approach, a cable harness production scenario was designed which involved routing two cables through different fixtures. A winding motion was also demonstrated by combining different manipulation primitives in a sequence. The video can be found here: <https://youtu.be/3Y5HFzrlxds>.

A. Contact Point Estimation

The accuracy of the DLO state representation relies on the identification of contact points through a Kalman filter. Therefore, we evaluate the uncertainty of this estimate for manipulation primitive D. To that end, the gripper equipped with the FT sensor was made to execute circular motions over the contact point to be estimated, and after a while a second fixture was placed in the path of the DLO, thus changing the contact point. Fig. 5 shows the position estimation error along the three dimensions.

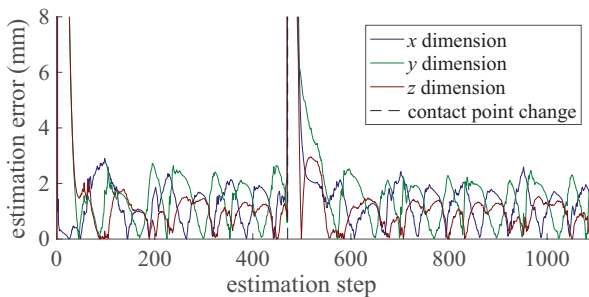


Fig. 5: The estimation error of the contact point along each axis. The vertical dashed line shows the moment when the contact point changes. For every 125 steps of the estimator, one full circle trajectory is executed.

Initially, the first contact point is accurately estimated already after half a circle. Once the contact point changes (at the dashed line), the estimate of the new contact point converges again after an initial spike in the error.

B. Manipulation Primitive Reliability

To evaluate the reliability of the proposed manipulation primitives, all were executed multiple times for randomized placement of the fixtures, initial position of the end effectors, as well as elasticity and length of the DLOs. The result of this evaluation is summarized in Fig. 4.

Most primitives had a perfect success rate, with a few exceptions. Primitives A and D had a combined total of three failures, due to a problem with the tension controller which also requires correct estimation of an elasticity parameter. This parameter is needed to maintain a constant tension on the DLO without triggering the YuMi's safety stop. In the first moment, the DLO was estimated to be significantly more elastic than it actually was, which caused a movement that quickly built up tension, reaching the limit of the robot. The failure of primitive C was due to an excessive distance between grippers which prevented the YuMi to be able to apply sufficient force and overcome the clipping resistance.

VI. CONCLUSION

We presented a DLO manipulation approach relying on FT sensing alone. This is feasible in applications which provide environmental contacts which limit the DLO's DOFs and enable tensioning. By keeping the DLO under tension, it is possible to estimate the location of these contacts, and therefore to keep a simplified path graph representation of the object's state. This representation was successfully employed to solve a cable harness problem. Future work will aim to complement FT sensing with visual information.

REFERENCES

- [1] M. Suomalainen, Y. Karayiannidis, and V. Kyrki, "A survey of robot manipulation in contact," *CoRR*, vol. abs/2112.01942, 2021.
- [2] A. Salem and Y. Karayiannidis, "Robotic assembly of rounded parts with and without threads," *IEEE Robotics and Automation Letters*, vol. 5, no. 2, pp. 2467–2474, 2020.
- [3] D. Almeida and Y. Karayiannidis, "Dexterous manipulation by means of compliant grasps and external contacts," in *IEEE/RSJ International Conference on Intelligent Robots and Systems*, pp. 1913–1920, 2017.
- [4] L. Manuelli and R. Tedrake, "Localizing external contact using proprioceptive sensors: The contact particle filter," in *2016 IEEE/RSJ International Conference on Intelligent Robots and Systems (IROS)*, pp. 5062–5069, 2016.
- [5] J. Sanchez, J. A. C. Ramon, B.-C. Bouzgarrou, and Y. Mezouar, "Robotic manipulation and sensing of deformable objects in domestic and industrial applications: A survey," *The International Journal of Robotics Research*, vol. 37, pp. 688 – 716, 2018.
- [6] J. Sanchez, K. Mohy El Dine, J. A. Corrales, B.-C. Bouzgarrou, and Y. Mezouar, "Blind manipulation of deformable objects based on force sensing and finite element modeling," *Frontiers in Robotics and AI*, vol. 7, p. 73, 2020.
- [7] D. Henrich, T. Ogasawara, and H. Worn, "Manipulating deformable linear objects-contact states and point contacts," in *Proceedings of the 1999 IEEE International Symposium on Assembly and Task Planning (ISATP'99)(Cat. No. 99TH8470)*, pp. 198–204, IEEE, 1999.
- [8] J. Acker and D. Henrich, "Manipulating deformable linear objects: characteristic features for vision-based detection of contact state transitions," in *Proceedings of the IEEE International Symposium on Assembly and Task Planning, 2003.*, pp. 204–209, IEEE, 2003.
- [9] J. Zhu, B. Navarro, R. Passama, P. Fraise, A. Crosnier, and A. Cherubini, "Robotic manipulation planning for shaping deformable linear objects with environmental contacts," *IEEE Robotics and Automation Letters*, vol. 5, no. 1, pp. 16–23, 2019.
- [10] J. Wittenburg, H. A. Richard, and J. Zierep, *Das Ingenieurwissen Technische Mechanik*. Springer-Verlag Berlin Heidelberg, 2014.
- [11] K. M. Lynch and F. C. Park, *Modern Robotics*. Cambridge University Press, 2017.